Maria STRĄKOWSKA, Robert STRĄKOWSKI
LODZ UNIVERSITY OF TECHNOLOGY, INST. OF ELECTRONICS
90-924 Łódź, Wólczańska 211/215 St.

Automatic eye corners detection and tracking algorithm in sequence of thermal medical images

Abstract

The article presents automatic eye corners detection algorithms in thermal images. Its target application is to perform quick and unnoticed measurement of human body temperature. It is proved that the temperature of eyes' corners is the most reliable and stable temperature considering infrared imaging. That measurements were done manually so far. Our approach is to do this automatically and create complete system for measurement of core human body temperature in crowded places where it is impossible to do this in another way (for example on the airport, railway station). Such system could prevent people for spreading off the epidemic. Two proposed algorithms are presented: first based on morphological operations and geometric features of human face, second based on the cross-correlation and idea of pattern tracking. The selection of appropriate ROI size for reliable temperature extraction was tested according to the distance to person under observation.

Keywords: eye corners detection, point tracking, IR thermography, thermal image processing.

1. Introduction

It has been proven lately, that the temperature in the corners of an eye represent very well the core temperature of the human body [1-2]. Therefore, the thermographic measurement can be used for massive screening e.g. at airports, railway stations, country boarders. These places are characterized with large movement of population. For that reason the temperature measurement in eyes corners should be done automatically and as fast as possible. Such detection system of people with higher body temperature could prevent from spreading serious diseases or epidemic outbreak.

Detection of face, eyes, mouth is widely described in the literature but mostly for visual images. In most cases methods used for automatic eye detection are based on gradient analysis, they use neural networks, templates, geometric features, morphological transformations, filtering, Hough transform and others [3-8]. The eye corner detection on thermal images is not so widely discussed in the literature [9]. Moreover, point tracking algorithm for infrared images is also significantly needed. For example when cold provocation approach is used in medical diagnosis [10] the test could last several minutes and the patient cannot sustain in the same position so long.

In this paper we present and compare these two algorithms based respectively on geometrical measurements and cross-correlation method.

2. Eye corner detection using geometrical features

The algorithm was designed for automatic detection of eyes corners in order to measure the core temperature of the human body using infrared camera [11-12]. For the first stage of the algorithm development and testing the uncooled microbolometer LWIR thermovison camera VarioCAM® hr research 600 Series, with the spatial resolution of 640×480 pixels and the spectral range of 7,5- 14 μm was used.

Human face detection is done by thresholding the image with a temperature level calculated with the Otsu's method [13]. It chooses the appropriate threshold in order to minimize the interclass variance of the black and white pixels. To improve the performance of face detection, the temperature threshold level is scaled by a factor that depends linearly on the average temperature value in the image. This allows to obtain satisfactory results in the most cases. Thus, obtained picture has more smaller regions and the facial area, due to the higher temperature, forms a single area easy for segmentation (Fig. 1).

Fig. 1. Original thermographic and binary image after binearization using Otsu method [9]

Additionally, in order to remove small objects, the operation of morphological opening is used with structuring element in the shape of a circle. After those operations only the pixels of detected human face are taken into account for further analysis.

Next the morphological image reconstruction followed by the dilatation of the image is done. These operations are used to smooth distribution and expand the areas of the high and low temperature. The temperature peaks are also suppressed. The resulting image is shown in Fig. 2. The greatest effect is seen in the areas of neck, nose, cheeks, around the mouth and above the eyes (eyebrows).

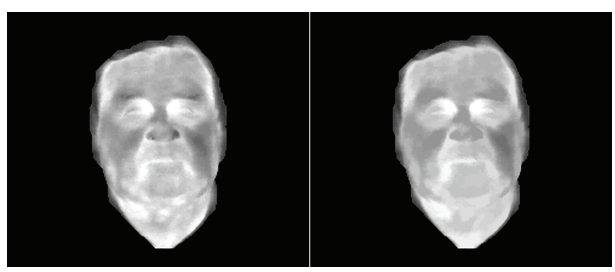

Fig. 2. Original image (left) and image after morphological reconstruction operations (right) [9]

In order to determine final regions of interest (ROIs) in thermal image the local maxima are localized. This operation is performed by subtracting two images: the output one from the previous step and the same after H-maxima transformation [14-15]. After this operation all regions of higher temperature within the face area are detected. The selection of the regions of interest is based on the assumption that the eyes position is fixed relative to the entire area of human face. For this purpose, an ellipse surrounding the face was determined on the thermogram. Knowing the position of the minor axis of the ellipse all regions of interest which are situated below this axis are deleted. Then the distances between the center of gravity of the ellipse, and the centers of gravity of the other regions of interest are calculated. Finally, the corners of the eyes are detected by selecting two regions, where the calculated distance is the smallest one. Additionally, in some cases, e.g. when the patient has unveiled neckline, ellipse surrounding the detected areas is stretched in the direction of the long diagonal. In this context, a further condition has to be fulfilled. If the ratio of the long axis of the ellipse to the shorter axis is greater than two, the threshold selection (the gravity center the regions of interest) is increased by a quarter of the length of the long axis of the ellipse. Selection takes place as in the previous case, by selecting two regions located above the minor axis of the ellipse.

If the number of remaining areas is less than two, the selected areas are located closest to a designated center of gravity regardless of whether the area is over or under a designated straight line.

The first eye's corners detection test was carried out on thermal images of children taken in the pediatric clinic. The set of 25 infrared images was analyzed (Tab. 1). The elevated body temperature in five thermograms.

The effectiveness of the algorithm was measured as the ratio of the number of automatically detected corners of the eyes to the total number of eyes' corners in investigated images. It was tested in a variety of settings, both the camera (distance) and a patient (position). Worst case scenario effectiveness, using only RAW images, was 84%. Due to the fact that the research is performed in the pediatric division two children were sitting on the lap of their parents. Implemented image segmentation did not work properly in this case, since the ellipse which surrounds the selected areas of interest included not only the child but also the adult. Therefore, it was necessary to crop manually the subimage with the person under test, as presented in Fig. 4. The effectiveness of the eyes' corners detection was then 92%. What is more, after cropping the face from thermograms for which the algorithm does not work due to the distance problem, the effectiveness was 100%.

To sum up, in most cases the algorithm worked correctly, as long as patients face images have been properly taken (no glasses, no other people in the FOV, uncovered head). Different temperature detected in each corner of the eye was often the result of bad position of the head. As the body temperature should be measured in corner of the eye, the human face should be situated perpendicularly to the optical axis of the. Both corners of eyes can be investigated in that position. With the fulfillment of this assumptions, the measurement is more accurate, and the effectiveness of the eyes' corners detection increases.

Tab. 1. Algorithm results – the values of temperatures in eye corners [9]

Image number	Temperature in eye 1 corner, °C	Temperature in eye 2 corner, °C	Automatically detected eye corners
1	35.00	35.25	2
2	36.75	36.49	2
3	36.77	36.46	2
4	36.76	37.27	2
5	37.27	37.15	2
6	37.09	37.38	2
7	35.54	35.72	2
8	35.41	35.41	2
9	36.52	36.74	0
10	36.08	36.38	2
11	37.20	37.20	0
12	36.89	36.69	2
13	36.02	35.98	2
14	35.96	35.96	1
15	37.49	37.24	2
16	35.90	35.54	2
17	35.73	35.87	2
18	37.51	37.70	0
19	35.79	35.71	2
20	35.82	35.57	2
21	36.50	36.74	2
22	36.49	36.49	1
23	34.77	34.61	2
24	35.13	35.32	2
25	34.99	34.79	2

The last step of the algorithm is to determine the human body temperature. It is calculated as average signal from Region Of Interest (ROI) which center position is determined by finding the maximum temperature in the determined eyes' corners regions. The size of the ROI to calculate the final body temperature should be selected accordingly to the parameters of used cameras and the distance to the person under investigation, what is presented precisely in the results section.

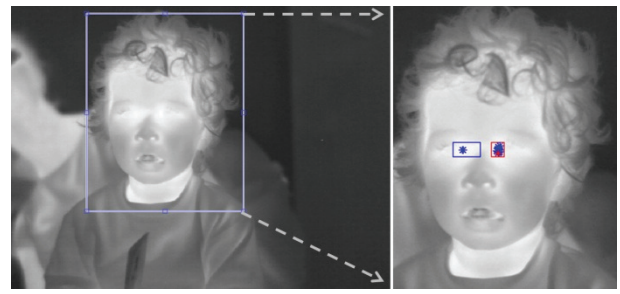

Fig. 4. Example of image on which there are two people in the camera field of view (left) and image after zooming (right) [9]

3. Eyes' tracking using cross-correlation

The idea of tracking the eye corners during the movement of the patient was also tested in this research. Such functionality of the systems can be useful in crowded places where sometimes it is hard to take an appropriate image where the corners of the eyes are well visible by thermovision camera. Using the sequence of the images the probability of extraction good body temperature increases. For the development and testing of this algorithms, due to technical issues, other thermovision camera was used: the cooled MWIR Cedip Titanium, with the spatial resolution of 640x512 pixels and the spectral range of 3,6-4,7 μm.

The algorithm is based on cross-correlation method [10]. The main assumption is that the image has the area with high gradient which can be easily found on the image or marked manually. For the purpose of finding the corners of the eye the region with eyes and nose is suitable. The subimage with high gradient is called Marker and full image is called Mask, presented in Fig. 3. Based on the cross-correlation methods, the Marker is found in every frame in the sequence. The corners of the eyes are detected as the pixels with the maximum values of temperature on the left and right side of the Marker (newly found for every frame). After that, the human body temperature value is calculated as average signal from eye's corners, the same way it was described for algorithm that uses face geometrical features.

The region of the Marker can be marked manually by the operator or automatically using first described algorithm for detection the corner of the eye. When the extraction of the Marker image is performed in the automatic way, the corners of the eye are detected. These two regions are connected and the Marker area is extended in every direction in order to cover the eyes and the nose.

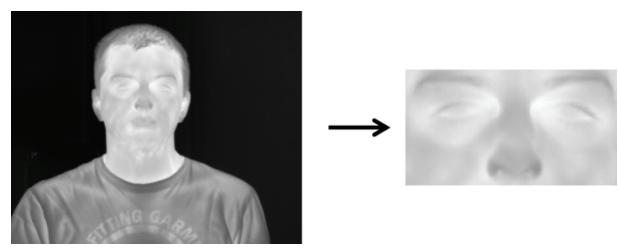

Fig. 3. First frame in the sequence of images (Mask) and its Marker image

4. Results

We compared two described algorithms in eye's corners tracking application. The tests were carried out on sequence of thermal images. Several experiments were performed and the functions of temperature in time from the region of eyes' corners were plotted. These experiments of eye corner tracking were performed using MWIR cooled camera, Cedip Titanium, with 25 frames/s rate. The image registration lasted almost 1 minute. The

selection of the ROIs appropriate size, from which values are averaged to measure body temperature, was also investigated.

The first algorithm (detection based on geometrical features) was applied independently for every frame in the sequence. The second algorithm tracks the Marker region (eyes and nose area) defined on the first frame of the sequence.

At first, the person under test moved sideways and inclined head with different angles and positions (Fig. 5). The results of body temperature measurement for both tracking algorithms, same eye corner and different size of ROI area are presented in Fig. 6, 7.

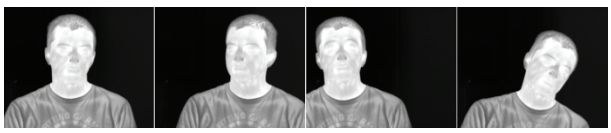

Fig. 5. The patient moves his head in different angles and positions (examples for 0 s, 5 s, 7 s and 60 s from the start of acqusition)

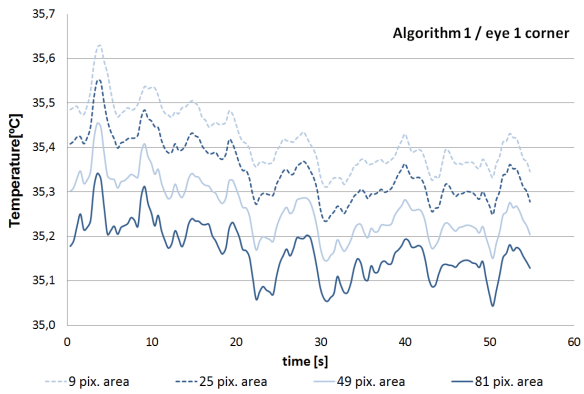

Fig. 6. The function temperature in time for algorithm 1, corner of eye 1 and for different size of region of interest

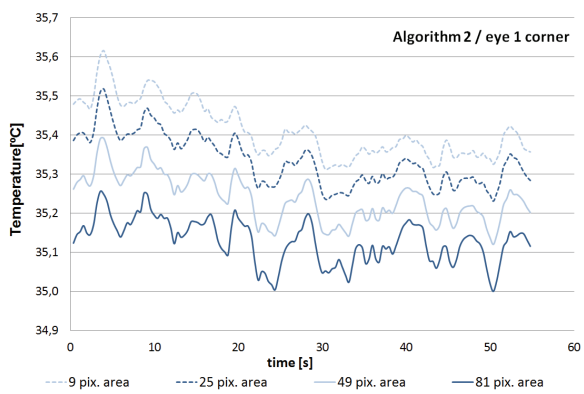

Fig. 7. The function temperature in time for algorithm 2, corner of eye 1 and for different size of region of interest

Tab. 2. The mean values of temperature from the sequence of images for different measurement methods

Number of pixels in ROI	9	25	49	81
Alg. 1 / Eye 1	35.4	35.4	35.3	35.1
Alg. 1 / Eye 2	35.9	35.8	35.7	35.5
Average value:	35.6	35.6	35.5	35.3
Alg. 2 / Eye 1	35.4	35.3	35.2	35.1
Alg. 2 / Eye 2	35.8	35.7	35.7	35.6
Average value:	35.6	35.5	35.5	35.4

The standard deviations and the extracted temperature values depending on the numbers of the pixels taking into ROI are shown in Tab 2. It is clearly seen that both algorithms manage to track the position of the eyes' corner with the same, sufficient precision. The shapes and value levels of plots from Fig. 6 and 7 correspond each other and the readout data have small value of standard deviation. The small variation in temperature is probably the effect of different position of the head and could be neglected.

Tab. 3. The values of temperature standard deviation the from the sequence of images for different measurement methods

Number of pixels	9	25	49	81
Alg. 1 / Eye 1	0.08	0.09	0.09	0.15
Alg. 1 / Eye 2	0.10	0.09	0.08	0.18
Average value:	0.09	0.09	0.09	0.17
Alg. 2 / Eye 1	0.09	0.09	0.10	0.11
Alg. 2 / Eye 2	0.11	0.10	0.08	0.08
Average value:	0.10	0.09	0.09	0.09

However, the values acquired from ROIs of different size are not the same. The larger the ROI area, the smaller the average measured temperature. This is a result of averaging bigger region around the hottest point in eye corner. Taking the parameters of the Cedip camera (the FPA size 9.6 mm×7.68 mm and 50mm lens) the real area of skin surface for different ROIs size and distances to target were calculated and presented in Tab. 4. The maximum dimensions of the real area on the skin to measure can be assumed as a square 3×3 mm. Even small changes in distance and ROI size can result in underestimation of measured body temperature, which is caused by measurement of the skin temperature outside eye corner. The measured temperature is also different in every eye corner (Fig. 8). It could be an effect of human physiology. The maximum measured temperature should be taken into consideration as a final result.

Tab. 4. The real size of the ROI area in eyes corners by Cedip Titanium camera for different ROI size and distance to target –dimensions in mm

Number of pixels in ROI	9	25	49	81
1 m from cam.	0.86 × 0.86	1.43 × 1.43	2.00 × 2.00	2.57 × 2.57
2 m from cam.	1.76 × 1.76	2.93 ×2.93	4.10 × 4.10	5.27 × 5.27
3 m from cam.	2.66 × 2.66	4.43 × 4.43	6.20 × 6.20	7.97 × 7.97
4 m from cam.	3.56 × 3.56	5.93 × 5.93	8.30 × 8.30	10.67 × 10.67
5 m from cam	4.46 ×x 4.46	7.43 × 7.43	10.40 ×10.40	13.37 × 13.37

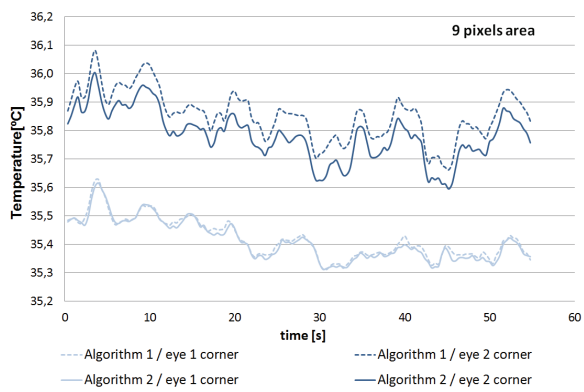

Fig. 8. The function temperature of time for both algorithms, both eyes and the size of region of interest 3×3 pixels (9 pixels area)

Last test was performed with the person moving towards and from the camera. The time graph of measured temperature is presented in Fig. 9. The distance changed from 4 m to 2 m (Fig 10). Comparing the results with the data in Tab. 4 it should be concluded that the size of ROI area must be chosen accordingly to the parameters of our system and distance to target. Inconsistency in this matter with the change of distance only along 2 m could lead to measurement error of 1°C and affects in passing the sick person.

The time to track/find eye's corners in one image (Intel i7 processor, same IR sequence) is comparable. On average it takes

around 130 ms for the first algorithm and 95 ms for the second one.

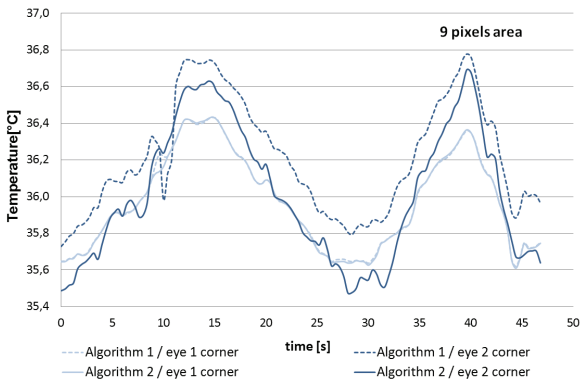

Fig. 9. The function temperature of time for both algorithms, both corners of eye, the size of region of interest 3×3 pixels and changing distance of object to the camera under examination (the curves for eye 1 corner are overlapping each other)

Fig. 10. The patient was changing the distance to the camera (examples for 0 s, 13 s, 30 s and 40 s from the start of acqusition)

5. Conclusions

Presented algorithms work correctly localizing the corners of the eyes and tracks them well in the sequence of images. The execution time of algorithm based on correlation is shorter than the algorithm based on the geometrical features. Moreover, correlation calculation can be speed up by searching the Marker only in the adjacent area of its last position.

The automatic eyes' corners detection algorithm should be improved by new preprocessing function. The problems with face localization in IR image due to not uniform background should be solved. This will allow to apply it in crowded places and group of people.

The fusion of two presented algorithms seems to be most suitable for eye's corners tracking in the sequence of infrared images. The eye's area should be detected by first algorithm and tracked by the second one. The main advantage of proposed method is the simplicity and the speed of operation. It is very important for the implementation of the algorithm in a real time system at potential sites of application eg. airports.

Moreover, to measure the human body temperature correctly, due to the small size of eye's corners and high temperature gradient around it, the appropriate size of the region should be calculated. This calculation must include the distance to the target and the infrared system's optical parameters. The measured human body temperature could be underestimated if ROI (in which the signal is averaged and measured) is too large for the setup of the system.

6. References

[1] Ring E.F.J., Jung A., Zuber J., Rutowski P., Kalicki B., Bajwa U.: Detecting Fever in Polish Children by Infrared Thermography. 9th International Conference on Quantitative InfraRed Thermography, Krakow, Poland, July 2-5, 2008.

[2] Ring E. F. J., McEvoy H., Jung A., Żuber J., Machin G.: New standards for devices used for the measurement of human body temperature. Journal of Medical Engineering & Technology, vol. 34, no. 4, May 2010, pp. 249–253.

[3] Rajpathaka T., Kumar R., Schwartz E.: Eye Detection Using Morphological and Color Image Processing, 2009 Florida Conference on Recent Advances in Robotics, FCRAR 2009.

[4] Peng K., Chen L., Ruan S., Kukharev G.: A Robust and Efficient Algorithm for Eye Detection on Gray Intensity Face, S. Singh et al. (Eds.): ICAPR 2005, LNCS 3687, pp. 302 – 308, 2005. Springer-Verlag Berlin Heidelberg 2005.

[5] Kong S. G., Heo J., Abidi B. R., Paik J., Abidi M. A.,: Recent advances in visual and infrared face recognition a review, Computer Vision and Image Understanding 97 (2005) 103–135.

[6] Peer P., Solina F.: An Automatic Human Face Detection Method, Computer Vision Winter Workshop, Ed. N. Brändle, pp. 122-130, Rastenfeld, Austria, February 1999.

[7] Saad A., Rosenfeld S., Rosenfeld A.: Eye detection in a face image using linear and nonlinear filters, Pattern Recognition, vol. 34, Issue 7, 2001, Pages 1367-1391.

[8] Budzan, S.: System detekcji twarzy i oczu w obrazach 2D z wykorzystaniem transformaty.

[9] Strakowska M., Strzelecki M.: Algorytm automatycznej detekcji kącików oczu w obrazach termowizyjnych, Pomiary Automatyka Kontrola, nr. 10, s. 1104-1107, 2011.

[10] Strakowska M., Strakowski R., Wiecek B., Strzelecki M.: Cross-correlation based movement correction method for biomedical dynamic infrared imaging, 11th International Conference on Quantitative InfraRed Thermography, 11-14 June 2012, Naples-Italy, ISBN 9788890648441.

[11] Nałęcz M.: Obrazowanie biomedyczne Tom 8., Akademicka Oficyna Wydawnicza EXIT, Warszawa 2003, ISBN: 83-87674-63-X.

[12] Więcek B., Strakowska M., Strakowski R., Strzelecki M., Wybrane biomedyczne zastosowania termowizji, Informatyka, Automatyka, Pomiary w Gospodarce i Ochronie Środowska, nr 1, 2011, str. 24-27.

[13] Otsu N.: A Threshold Selection Method from Gray-Level Histograms. IEEE Transactions on systems, Man, And Cybernetics, vol. SMC-9, no. 1, January 1979.

[14] Vincent L.: Morphological Gray scale Reconstruction in Image Analysis: Applications and Efficient Algorithms, IEEE Transactions on image processing, vol. 2, no. 2, April 1993.

[15] Soille P.: Morphological Image Analysis: Principles and application Second Edition, ISBN 3-540-42988-3 Springer-Verlag Berlin Heidelberg New York, 2002, s.203-206.

Received: 12.03.2015 *Paper reviewed* *Accepted: 05.05.2015*

M.Sc. Maria STRĄKOWSKA

She graduated the Faculty of Electrical, Electronic, Computer and Control Engineering Lodz University of Technology, majoring in Electronics and Telecommunications, specialty Images and Signal Processing. In 2010, she began doctoral studies. Her research interests focus around the thermographic image processing methods, the problems of thermal measurements and modeling of thermal phenomena.

e-mail: maria.strakowska@dokt.p.lodz.pl

M.Sc. Robert STRĄKOWSKI

Robert Strakowski graduated from the Faculty of Electrical, Electronics, Computer and Control Engineering Lodz University of Technology. He is co-author of 7 publications and one chapter in the book. In The Department of Electronic Systems and Thermography he conducts research on the new method of signal correction from uncooled bolometers detectors. His research interests also include thermographic imaging and artificial neural networks.

e-mail: robert.strakowski@p.lodz.pl